

Journal of

www.biophotonics-journal.org

BIOPHOTONICS

WILEY-VCH

REPRINT

FULL ARTICLE

A comparative evaluation of diffuse reflectance and Raman spectroscopy in the detection of cervical cancer

Rubina Shaikh**,¹, Vasumathi G. Prabitha**,², Tapas Kumar Dora³, Supriya Chopra³,
Amita Maheshwari⁴, Kedar Deodhar⁵, Bharat Rekhi⁵, Nita Sukumar²,
C. Murali Krishna*,¹, and Narayanan Subhash*,⁶

¹ Chilakapati Laboratory, ACTREC, Kharghar, Navi Mumbai 410210, India

² Biophotonics Laboratory, National Centre for Earth Science Studies, Akkulam, Thiruvananthapuram – 695 031, Kerala, India

³ Tata Memorial Center, Radiation Oncology, ACTREC, Kharghar, Navi Mumbai 410210, India

⁴ Tata Memorial Hospital, Gynecology Oncology, Parel, Mumbai 400012, India

⁵ Tata Memorial Hospital, Surgical Pathology, Cytopathology, Parel, Mumbai 400012, India

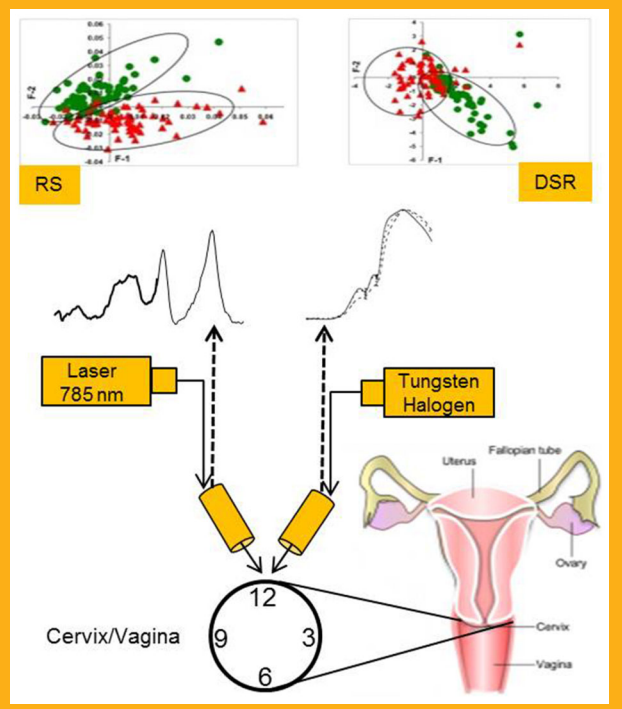
⁶ Sascan Meditech Pvt Ltd, Centre for Innovation in Medical Electronics, BMS College of Engineering, Basavanagudi, Bangalore – 560019, India

Received 18 September 2015, revised 13 January 2016, accepted 25 January 2016

Published online 27 February 2016

Key words: Raman spectroscopy, diffuse reflectance spectroscopy, *in vivo*, cervical intraepithelial neoplasia, principal component-linear discriminant analysis, cancer screening

Optical spectroscopic techniques show improved diagnostic accuracy for non-invasive detection of cervical cancers. In this study, sensitivity and specificity of two *in vivo* modalities, i.e diffuse reflectance spectroscopy (DRS) and Raman spectroscopy (RS), were compared by utilizing spectra recorded from the same sites (67 tumor (T), 22 normal cervix (C), and 57 normal vagina (V)). Data was analysed using principal component – linear discriminant analysis (PC-LDA), and validated using leave-one-out-cross-validation (LOOCV). Sensitivity, specificity, positive predictive value and negative predictive value for classification between normal (N) and tumor (T) sites were 91%, 96%, 95% and 93%, respectively for RS and 85%, 95%, 93% and 88%, respectively for DRS. Even though DRS revealed slightly lower diagnostic accuracies, owing to its lower cost and portability, it was found to be more suited for cervical cancer screening in low resource settings. On the other hand, RS based devices could be ideal for screening patients with centralised facilities in developing countries.



* Corresponding authors: e-mail: pittu1043@gmail.com, mchilakapati@actrec.gov.in, subhashnarayanan@gmail.com

** These authors contributed equally to this work.

1. Introduction

Cervical cancer is the leading cause of cancer related deaths among women population in developing countries. The routine Papanicolaou (Pap) test, which is considered as a specific test for high-grade lesions is moderately sensitive. Cervix with abnormal Pap smear is further evaluated by colposcopy directed biopsy, which is a relatively invasive procedure and is subjective [1]. Histopathology, the gold standard of diagnosis, is a time-consuming process and skilled pathologists are needed for an accurate diagnosis [2]. Constraints of cytology-based tests in low-resource settings have led to the use of visual screening tests, such as visual inspection with acetic acid (VIA) and visual inspection with Lugol's iodine (VILI) for cervical cancer screening [2]. These tests are also subjective as they rely on visual examination and interpretation of pathology slides needs to be carried out by trained histopathologists. Human papilloma virus (HPV) vaccines protect only against major high-risk HPV types (16 and 18), that cause approximately 70% of cervical cancers, and in resource limited settings, widespread implementation of HPV vaccines is critically challenged by its cost and lack of appropriate infrastructure [1].

Therefore, development of alternate modalities with adequate accuracies, less complexity/cost and least side effects is necessary for cervical screening. Optical spectroscopic techniques are being developed over the last few decades with a strong emphasis for *in vivo* cancer screening and real-time diagnosis of the grade of malignancy [3, 4]. Wide variety of spectroscopic techniques, including diffuse reflectance, fluorescence and Raman spectroscopy, offer real-time assessment of biochemical and morphologic changes in tissue composition during carcinogenesis in various organ sites [3, 4]. The utility of these techniques in clinical settings lays in their ability for real-time, non-invasive, and objective interpretation, which make these techniques viable options among the women population in many low-resource countries.

Raman spectroscopy (RS) relies on inelastic scattering of light, a unique technique capable of label-free and non-destructive probing of cellular molecules, for example to determine highly specific diagnostic molecular fingerprints [5–8]. RS has been widely used for clinical diagnosis of different types of cancers, such as oral, skin, breast, gastro intestinal tract, cervix, bladder, prostate and lung [6, 9, 10]. Mahadevan et al. recorded the first *in vivo* and *in vitro* Raman spectrum of cervical tissues in 1998 [11, 12]. Following *in vivo* cervical cancer studies demonstrated resemblance between *in vivo* and *in vitro* cervix spectra [13]. Subsequent studies explored the classification of high-grade dysplasia, low-grade dysplasia and benign conditions as well as classification among normal ectocervix and endocervix [14, 15]. It

was noticed that insertion of parameters like hormonal and menopausal status, could improve the classification efficiency [16]. *In vivo* precancer detection utilizing high wave-number Raman spectra as well as the application of simultaneous fingerprint in enhancing diagnostic accuracies for detection of cervical precancer has been reported [17,18]. A number of studies have shown Raman spectroscopy as a powerful tool with remarkable diagnostic performance for detecting cervical cancers [19–23].

In comparison, diffuse reflectance spectroscopy (DRS), which is an elastic scattering process, is sensitive to changes in tissue morphology, vasculature, and chromophores. Many investigators have explored the potential of DR spectroscopy for noninvasive and real time detection of oral cancer, ovarian cancer, cervical cancer, breast cancer, and bladder cancer [24–35]. Mourant et al. detected precancerous and cancerous cervical lesions using a probe designed to collect polarized and unpolarized diffusely reflected light [36]. In a study to discriminate cervical lesions, Chang et al. reported that fluorescence has better performance as compared to reflectance and a combination of both techniques gave a modest improvement in diagnostic performance [30]. Georgakoudi et al. developed a technology called trimodal spectroscopy (TMS), combining intrinsic fluorescence, diffuse reflectance and light scattering spectroscopy for analyzing squamous intraepithelial lesion (SIL) of the cervix with improved diagnostic accuracies [31]. Most of these studies using DR spectroscopy for cervical cancer screening were based on the reduction in the intensity of diffusely reflected white light.

In 2006, Subhash et al. proposed the use of the ratio of oxygenated haemoglobin absorption dips at 545 nm and 575 nm (R_{545}/R_{575}) in the diffusely reflected white light for detection of oral cancer, which was later validated through a clinical trial to discriminate dysplastic oral lesions from hyperplasia with a sensitivity of 100% and specificity of 86% and grade tissues [24, 25]. Later, Mallia et al. found this DR ratiometric technique to be very effective for discriminating various grades of tongue cancer, where laser-induced autofluorescence (LIAF) technique had very low diagnostic accuracies [37]. Jayanthi et al. reported enhanced diagnostic accuracies for grading the oral lesions using multivariate statistical techniques involving PCA and LDA and compared these with the results obtained from analysis of LIAF spectra recorded from the same tissue [26, 38]. Recently, Prabitha et al. has utilized PCA and LDA on the DR spectra recorded *in vivo* from 34 patients and reported a sensitivity of 89% and specificity of 97% for discriminating high-grade SIL from normal and 100% sensitivity and specificity for discriminating HSIL from LSIL [39].

During the last few decades, a number of promising non-invasive optical imaging techniques have

emerged for screening and diagnosing of cervical cancers. A multimodal hyper-spectral imaging device that collects and analyses both fluorescence and reflectance spectra from the cervix *in vivo* was able to detect CIN with improved accuracy as compared to a simultaneously obtained Pap smear [40]. Hyperspectral imaging can be utilized in prescreening of liquid-based Pap test slides to improve the efficiency in Pap test diagnoses and the system identified normal cervical cells from high grade precancerous cells with a sensitivity 93.5% and specificity of 95.8% [41].

Prabitha et al. has recently carried out a clinical study by recording the diffuse reflectance (DR) images of cervix at the oxygenated haemoglobin absorption peaks of 545 nm and 575 nm [42]. It was observed that the reflectance image intensity ratio R545/R575 could non-invasively discriminate healthy tissue from premalignant and malignant lesions in real-time. Also, advances in electronics and computerised technology have led to miniaturisation of CCDs and spectrometers and to smart phone based diagnostic techniques and microendoscopy systems with lower cost and complexities. Yu et al. has reported an innovative and smart fiber-optic probe to eliminate operator bias, reduce size and power consumption, which noninvasively quantifies the optical properties of epithelial tissues and detects precancerous changes in the cervix and oral cavity [43]. Pierce et al. has reported a low-cost, high-resolution microendoscope (HRME) imaging system, which was used in a pilot study to evaluate epithelial cell morphology *in vivo* and to detect various grades of cervical cancer *in vivo* [44]. The results of this study suggest that evaluation of suspicious lesions by HRME may assist in ruling out immediate cryotherapy, thereby increasing the efficiency of current see-and-treat programs. Also, there are advances with regard to incorporation of spectroscopic sensors capable of measuring the optical spectrum of a physical object in a mobile communication device [45]. But these devices have only limited applications as their sensitivities do not match with those of other optical spectroscopy and imaging based devices.

The choice of any modality for practical application in a clinic would depend on various factors, such as diagnostic accuracy, size of the device, ease of use, affordability and to what extent it meets the un-

met need of the clinician. All the above studies show that DRS and RS are good techniques for cervical cancer detection. But, all those studies were carried out in different clinical environments in different cohort of patients and the spectral data were analysed using different statistical techniques. Therefore, it is important to understand the relative merits of these modalities for patient screening by carrying out a clinical study using these two modalities on the same set of patients in the same clinical setting.

In this clinical study, we have recorded the *in vivo* DR and Raman spectra sequentially from the same sites of patients using instruments developed in two different laboratories. The recorded spectra were analysed for the discrimination of cervical tumors from normal by using multivariate statistical techniques viz., Principal Component Linear Discriminant Analysis PC-LDA. The results obtained were cross validated using the leave-one-out method and the diagnostic accuracies are presented.

2. Materials and methods

2.1 Study population

The study population included a total of 26 subjects (20 cases with tumor cervix (T) and 6 normal cervix (N) cases with non-cervical gynaecological cancers, such as ovarian and breast cancers, but with a healthy cervix). The study was carried out at Advanced Centre for Treatment Research and Education in Cancer (ACTREC) and Tata Memorial Centre (TMC), Mumbai. The protocol to acquire *in vivo* DR and Raman spectra was reviewed and approved by the Institutional Ethics Committee of ACTREC and TMC. After explaining the details of the procedure, an informed and written consent was obtained from each participating patient before initiating any study related procedures. A total of 67 tumor spectra (T) were acquired from pathologically certified sites of 20 cervical cancer subjects, 22 normal cervix spectra (C) were collected from normal cervix sites from 6 non-cervical cancer subjects and 57 normal vaginal spectra (V) were recorded from 20 subjects (Table 1). Since normal vaginal sites (V)

Table 1 Details of samples: tumor cervix (T), normal cervix (C), normal vaginal sites (V).

Categories	No. of cases	No. of spectra	2 tier classification
Cervical tumor (T)	20	67	67 Tumor (T) sites
Normal Cervix (C)	6	22	
Normal Vagina (N)	20	57*	79 Normal (N) sites

*Out of 57 normal vaginal spectra, 14 spectra (5 cases) were recorded from normal cervix case and 43 spectra (15 cases) from cervical tumor cases.

can be used as an internal control [21], we clubbed the normal cervix spectra (C) and normal vaginal spectra (V) into one category as 'Normal' (N). Thus the study involved a total of 67 tumor spectra (T) and 79 normal spectra (N) as shown in Table 1. The DR and Raman spectra collected from the same sites of the patients only were used for spectral analysis and comparison.

2.2 DR spectroscopic system

The schematic of the DR system used for point monitoring of cervical tissue is shown in Figure 1. The system consists of a tungsten halogen lamp (Model: LS-1-LL, Ocean Optics, USA), which provides a broad band white light for illumination of tissue and a miniature fiber-optic spectrometer (Model: USB 4000 FL VIS-NIR, Ocean Optics, USA) connected to the USB port of a laptop computer, loaded with a spectrometer operating software, SpectraSuite (Ocean Optics Inc, USA) for recording of spectra. The excitation light from the lamp is coupled to one arm of a bifurcated optical fiber assembly (Model: ZR400-5-VIS/NIR, Ocean Optics, USA) made of fused silica with a core diameter of 400 μm and numerical aperture (NA) of 0.22. The diffusely reflected light from the tissue is collected by the 6 collection fibers surrounding light delivery fiber and sent to the spectrometer through the other arm of the bifurcated fibre assembly. The fibre assembly ends in a steel ferrule of 6 mm diameter and 18 cm length, with a disposable PVC black sleeve of 2 cm length inserted at its tip that maintains an optimal distance (3 mm) between tissue surface and probe tip. The spectrometer was operated with an integration time of 100 ms, a boxcar width of 10 nm and number of scans of 40, for improved signal to noise

ratio (S/N). Before acquiring the data, spectra were corrected for background light by recording a background spectrum, which was automatically subtracted from the recorded spectrum using SpectraSuite. Three to four spectral recordings were taken in the wavelength range 350–750 nm from each site and the averaged spectra was used for analysis after intensity normalization.

2.3 Raman spectroscopic system

Raman spectroscopic system used in the study is illustrated in earlier reports [22]. This system consisted of a diode laser emitting at 785 nm (Model PI-ECL-785-300-FC, Process Instruments), and a high-efficiency spectrograph (Model HE-785, Jobin-Yvon-Horiba, France) with fixed 950 gr/mm grating and a charge coupled device (CCD-1024X256-BIDD-SYN, Synapse, France). The commercial Raman probe (Model RPS 785/12-5, In Photonics Inc., Downey St., Norwood, Massachusetts, USA) used to couple the laser source and the detection system consisted of an excitation fiber of 105 μm diameter and a collection fiber of 200 μm diameter. As per the manufacturer's specifications, the numerical aperture, estimated spot size, depth of penetration and spectral resolution of probe were 0.40, 105 μm , 1 mm and 4 cm^{-1} , respectively. To maintain the focus during measurements, a detachable spacer with a length of 5 mm was attached at the tip of the probe. All the Raman spectra were acquired at 80 mW laser power, integrated for 5 s, and averaged over three accumulations.

In vivo Raman Spectra were pre-processed and corrected for CCD response using National Institute of Standards and Technology (NIST) certified Standard Reference Material 2241 (SRM 2241) [46]. This

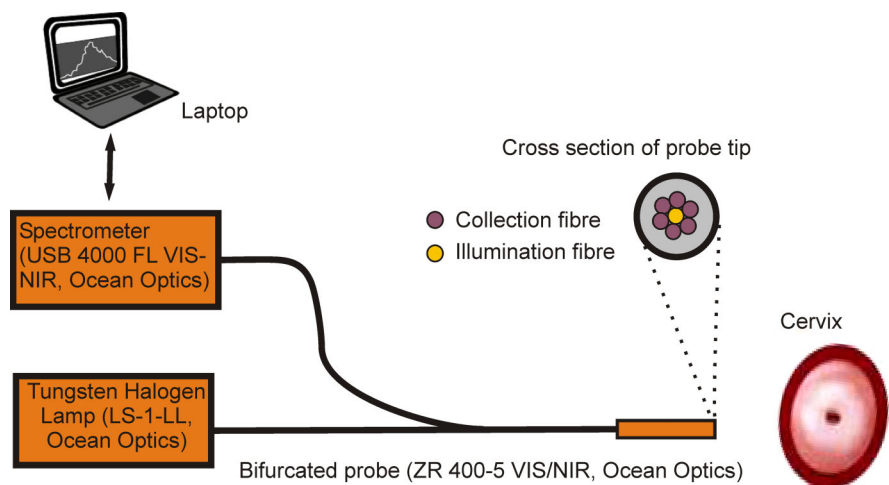


Figure 1 Schematic of DR spectroscopic point monitoring system used in the study.

was followed by subtraction of background signals for optical elements and CaF₂ window. First derivatives of spectra (Savitzky–Golay method, window size-3) were computed to remove interference of the slow moving background [47, 48]. Since our previous cervical cancer studies have demonstrated the efficacy of the 1200–1800 cm⁻¹ region in classification and it is less influenced by fiber signals, we have employed same region for analysis [21]. Background corrected spectra were interpolated and first derivatized followed by a vector normalization. Vector-normalized spectra were subjected to the multivariate statistical tool PC-LDA using algorithms implemented in MATLAB® (Mathworks Inc., Norwood, Massachusetts) based in-house software [49].

Average Raman spectra were computed from the background subtracted spectra (without derivatization) for each group, followed by baseline correction by fitting a fifth order polynomial.

2.4 Data collection

To avoid contamination among subjects, prior to spectral recording, the DR probe and the spacer (tip of Raman probe) were disinfected with CIDEX (Johnson and Johnson, Mumbai, India) solution and Raman probe was wrapped in parafilm sheet. Raman probe was advanced through the speculum and placed in contact with all four quarters of the cervix of each patient and approximately 2–3 Raman spectra were recorded from each site. The average of these spectra represents the spectral signature corresponding to that site. The measurement is then repeated using the DR probe from the same site and the average DR spectra is recorded. Abnormal bleeding was present in a few cases and some of the spectral data profiles from such sites were extremely bad and four such cases were excluded from further analysis. In this study, we have used only the spectra recorded corresponding to common sites using both DR and Raman probes.

2.5 Statistical techniques

Although there are several multivariate statistical tools, such as artificial neural network (ANN), hierarchical cluster analysis (HCA), and principle components analysis (PCA) available for data analysis, it is necessary to choose one that is rapid and provides a simple discriminating algorithm from the clinician's point of view. We have found that multivariate statistical analysis involving Principal Component – Linear Discriminant Analysis (PC-LDA) provides reasonably good results. In PC-LDA meth-

odology, PCA is initially carried out on the data set to reduce the data dimensionality while preserving the diagnostically data significance for classification. PCA describes data variance by identifying a new set of orthogonal features, called as principal components (PCs) or eigenvectors. Due to their orthogonal characteristics, the first few PCs are sufficient to represent maximum data variance. The unpaired Student's *t*-test is used to identify diagnostically significant PCs ($p < 0.05$). These PC scores are then used as input for LDA based classifications. Thus, Principal component analysis explores the full spectrum information without any intuition with regard to the origin of spectral differences and LDA has been used to extract discriminant scores by maximising their between-class variability for objective discrimination between normal and tumor conditions. PC-LDA analysis of Raman data were carried out using above mentioned home built software and the statistical software SPSS version 16.0 for Windows was employed for DR data. The scree plot of DR data was drawn manually using Origin 6.0 software.

Considering vagina as an internal control, the data set (79 normal sites (N) and 67 cervical tumors (T)) were normalised and multivariate statistical techniques PC-LDA, were carried out separately to develop diagnostic algorithms for the differentiation of tumors from normal cervical tissue. PCA was conducted on the normalized spectral data to generate PC scores. The PCs for which the eigen values are greater than or equal to one were retained. The most diagnostically significant PCs ($p < 0.05$) were selected as input for the development of linear discriminant functions that maximizes the variances in the data between groups. The loading factors calculated for each subjects were used to create a scatter plot. The significant PCs derived were used as input variables of LDA for classifying the groups as normal and tumor tissue by generating a discriminant function. LDA provided data classification and diagnostic accuracies, such as Sensitivity (Se), Specificity (Sp), Positive Predictive Value (PPV) and Negative Predictive Value (NPV). The performance of the PC-LDA diagnostic model was further validated by leave-one-out cross validation (LOOCV). The diagnostic accuracies were compared for both Raman and DR based diagnostic algorithms.

3. Results and discussion

Photons propagating in biological tissue experience various events, such as transmission, reflection, absorption, fluorescence and scattering. After multiple elastic scattering due to heterogeneity in the refractive index of the tissue components, some of these photons get diffusely reflected back carrying infor-

mation on tissue composition and morphology, which is useful for cancer diagnostics [50]. Changes associated with malignant transformation are increase in epithelial thickness, nuclear size and nuclear to cytoplasmic ratio, along with changes in the nuclear chromatin texture and collagen content in the stroma, and angiogenesis [28, 34, 51]. In the visible band, dominant absorbers in oral and cervical tissues are oxygenated hemoglobin (HbO_2) and deoxygenated hemoglobin (Hb). It is well known that the heme synthesis is disturbed in malignant tissues due to the reduced activity of the ferrochelatase enzyme, which results in lower haemoglobin production and correspondingly lower absorption at 545 nm and 575 nm of the oxygenated haemoglobin spectra [52]. As observed by Amelink et al. and Lovat et al., we also have noticed that oxygenated hemoglobin absorption dips at 545 nm and 575 nm are more prominent in healthy cervix as compared to malignant tissues [53, 54]. Furthermore, cervical cancer tissues show significantly lower DR intensities compared to normal cervical tissue, as in the case of oral cavity tissues.

Raman spectroscopy is an advanced spectroscopic tool for molecular fingerprinting and is sensitive to the biomolecular changes associated with malignancy. The scattered energy corresponds to the specific Raman active vibrational modes of the biomolecules and the inelastic scattered light therefore represents a molecular “fingerprint”. The shape, position and relative intensity of the bands in the Raman spectrum carry information about the molecular composition of the sample [55]. As reported earlier, we observed collagenous features in normal cervix spectra, and non-collagenous and nucleic acid features in tumor spectra [11, 21, 22, 56, 57].

Socio-cultural perception about screening tests, modesty, and lack of encouragement from family member and lack of awareness inhibit women from screening tests. They come for treatment only when the symptoms reach a severe stage in cancer development. So it was not easy to get healthy controls in our clinical study and since vagina and cervix (ectocervix) are known to have similar histology, we have used spectral readings from normal vagina as an internal control [21, 58].

In an *in vivo* study to detect cervical cancer using Raman spectroscopy, Rubina et al. has explored the utility of the vagina as an internal control [21]. In that study, the spectral features of normal cervix and vaginal controls in cancerous and noncancerous subjects were found to be similar. PC-LDA of tumor, normal cervix, and vaginal controls further supported the utility of using the spectra recorded from vagina as an internal control and reported 97% classification efficiency between normal (N) and cervix tumor (T).

3.1 DR and Raman spectral features

Figure 2 shows DR spectra of cervical tumor (T), normal cervix (C) and normal vaginal sites (V) in the spectral region of 450–750 nm, normalized to its maximum intensity. Marked variation was observed between the normal (N) and tumor (T) spectral signatures. It can be seen that the intensity of the oxygenated haemoglobin absorption dips are more prominent in normal (N) than in tumor cervix sites (T). Overall intensity reduction is seen in the spectrum from the cervical tumor (T). Changes noticed in the line shape and intensity of DR spectra is mainly due to absorption by haemoglobin, which is the dominant absorber in the visible range of the spectrum.

Vector-normalized mean *in vivo* Raman spectra of cervical tumor (T), normal cervix (C) and normal vaginal sites (V) along with their standard deviations are illustrated in Figure 3. Standard deviation spectra exhibited minor intensity related changes within groups. The mean Raman spectra of tumor (T) exhibited strong and sharper amide I, a slight shift in δCH_2 and a distinct band at 1340 cm^{-1} , which are indicative of nucleic acid and non-collagenous proteins. Whereas, the average Raman spectra of a normal cervix (N) showed characteristic features of amide III and strong and broad amide I. These features can be attributed to the presence of collagenous proteins. The spectral findings corroborate previous Raman spectroscopic studies on cervical cancers [11, 21–23, 56, 57]. Even though *in vivo* vagina spectral (V) features were very similar to normal

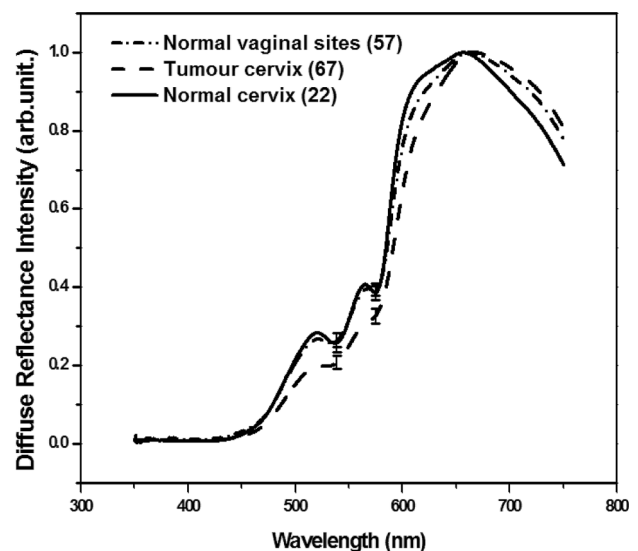


Figure 2 Average, normalized diffuse reflectance (DR) spectra of cervix tumor (T) sites, normal cervical (C) sites and normal vaginal (V) sites with their standard deviations shown at 545 and 575 nm.

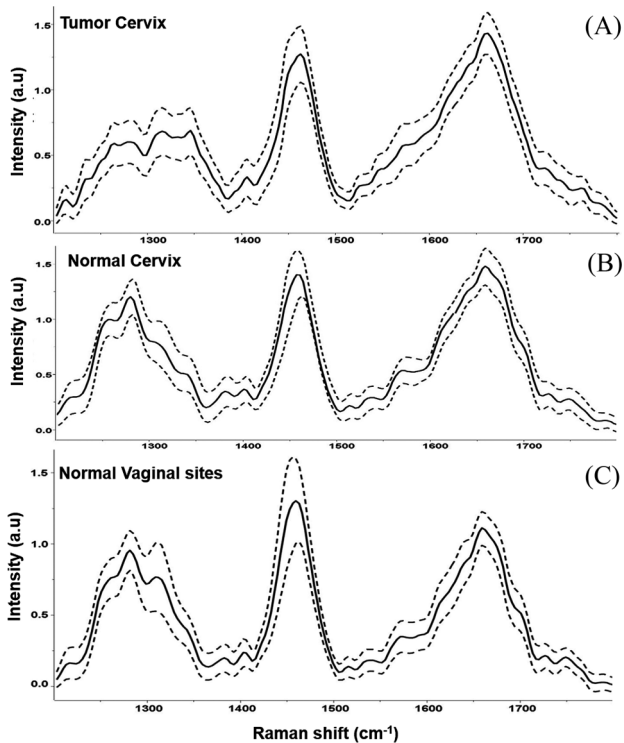
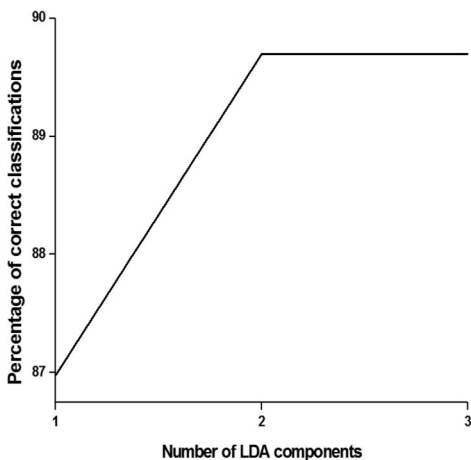
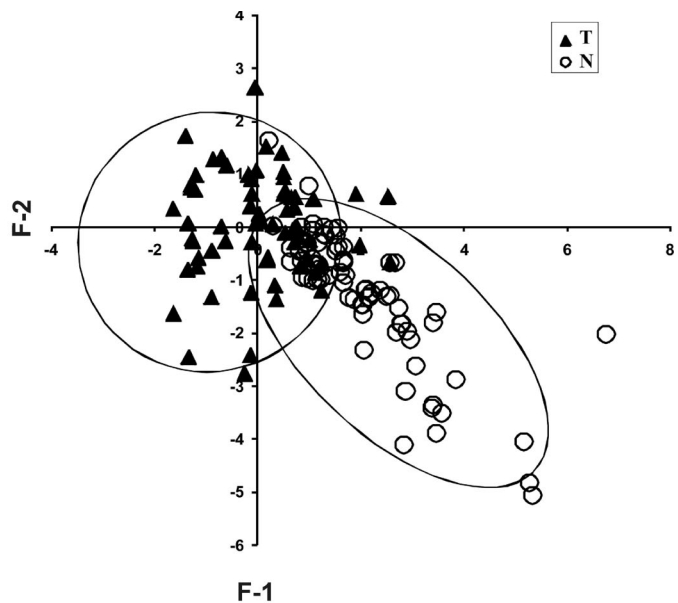


Figure 3 Average, normalized Raman spectra (RS) of (A) cervical tumour (T), (B) normal cervical (C) sites and (C) normal vaginal (V) sites with their standard deviations.

cervix (C) and exhibited features of collagenous proteins, they showed resemblances in their biochemical compositions to that of normal cervix sites.



(a)



(b)

Figure 4 Classification of tumour (T) and normal (N) cervix and vaginal sites based on DR data; (a) correct percentage of classification with LDA components and (b) scatter plot.

3.2 Statistical analysis of DR and Raman data

PCA-LDA analysis was carried out on the high dimensional trained DR and Raman preprocessed spectral data set consisting of 79 normal (N) and 67 cervical tumor (T) sites. During PCA-LDA for DR, three LDA components exhibited 90% classifications whereas, for RS the three components contributed to 94% classification, as shown in scree plots (Figures 4a, 5a), which depicts the variance or percent correct classifications accounting for the total number of factors selected for DR and Raman analysis. The extracted PCs were able to differentiate the two groups at large. Loading factors were used and the scatter plots were drawn (Figures 4b, 5b) depicting exclusive clusters corresponding to DR and Raman data of normal (N) and cervical tumors (T). LOOCV was also executed to evaluate the classification efficiency of the model and the results are given in Table 2.

3.3 Classification accuracy of DR and RS

Table 2 shows PCA-LDA classification and leave one out cross validation results of both DR and Raman spectral data. As seen in Table 2, 4/79 normal sites (N) and 10/67 tumor sites (T) were misclassified in the standard set for DR data and in the validation data set 5/79 normal sites (N) and 10/67 (T) tumor

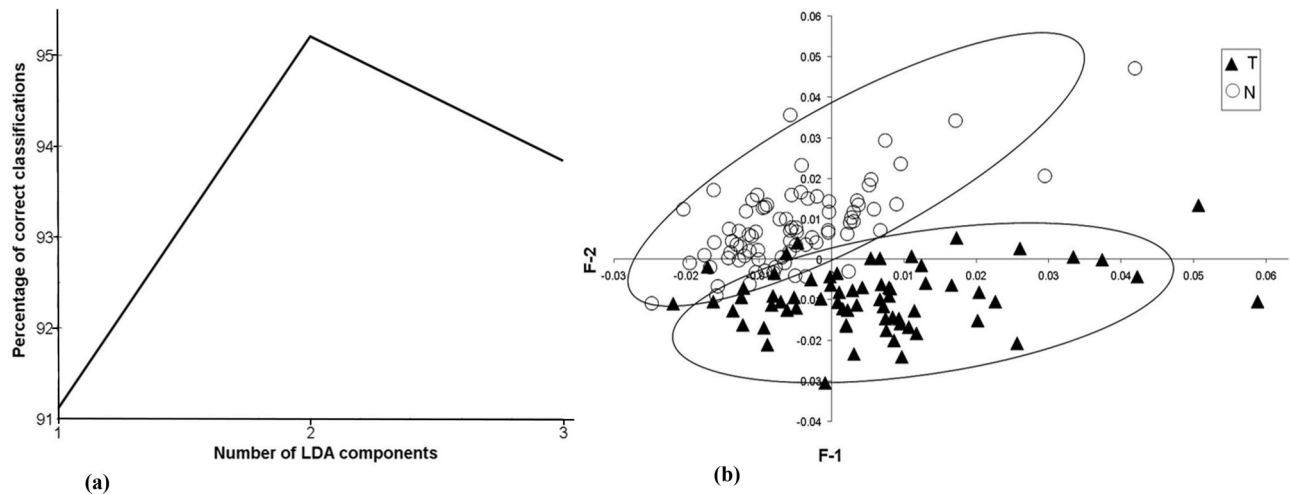


Figure 5 Classification of tumour (T) and normal (N) cervix and vaginal sites based on Raman data; (a) correct percentage of classification with LDA components and (b) scatter plot.

sites were misclassified. In comparison, 3/79 normal sites (N) and 6/67 tumor sites were misclassified in the Raman data set. Whereas, in the validation data set, 4/79 normal sites (N) and 6/67 tumor sites (T) were misclassified. The diagnostic accuracies for distinguishing tumor (T) from normal tissue (N) sites were calculated separately for both data sets and are shown in Table 3. Sensitivity, specificity, positive predictive value (PPV) and negative predictive values (NPV) were 91%, 96% and 95% and 93%, respectively for Raman data set and 85%, 95%, 93% and 88%, respectively for DR data. Specificity and PPV were comparable for DR and RS, whereas sensitivity and NPV were slightly lower for DR as compared to RS.

Table 2 Principal component-linear discriminant analysis; (a) standard models, and (b) leave-one-out cross-validation of tumor cervix (T) and normal sites (N) for DR and Raman data.

	Normal (N)	Tumor (T)
Raman Spectroscopy		
(a) Standard Model		
Normal (N)	76	3
Tumor (T)	6	61
(b) Leave-One-Out-Cross-Validation		
Normal (N)	75	4
Tumor (T)	6	61
Diffuse Reflectance Spectroscopy		
(a) Standard Model		
Normal (N)	75	4
Tumor (T)	10	57
(b) Leave-One-Out-Cross-Validation		
Normal (N)	74	5
Tumor (T)	10	57

In this study, the diagnostic accuracies obtained using DRS are significant and comparable with Raman studies. In literature, there are several reports distinguishing normal and cancerous cell specimens *in vivo* and *ex vivo* using DR spectroscopy. Based on principal-component analysis and Mahalanobis distance classification, Mirabel et al. discriminated squamous normal from high-grade squamous intraepithelial lesions with a sensitivity of 72% and a specificity of 81% and distinguished columnar normal epithelium from high grade dysplasia with a sensitivity of 72% and specificity of 83% by analyzing reflectance spectra *in vivo* [28]. Chang et al. reported a sensitivity and specificity of 83%, and 80%, respectively per patient for the detection of cervical pre-cancer based on a combination of reflectance and fluorescence spectroscopy [30]. Using logistic regression and leave-one-out validation, Georgakoudi et al. reported that trimodal spectroscopy was able to detect SIL from non-SIL with a sensitivity and specificity of 92% and 71%, respectively [31]. In comparison, we have obtained a sensitivity and specificity of 85% and 95%, respectively for discriminating tumor (T) from normal (N) cervical sites.

Kanter et al. have reported an overall accuracy of 94% to detect cervical dysplasia using Raman spectroscopy by incorporating a woman's hormonal status [16]. The diagnostic algorithms based on prin-

Table 3 Diagnostic accuracies for Raman and DR data.

Diagnostic accuracies	Raman studies (%)	DR studies (%)
Sensitivity	91	85
Specificity	96	95
Positive predictive value	95	93
Negative predictive value	93	88

principal component analysis and linear discriminant analysis together with the leave-one-patient-out cross-validation method on high wave number Raman spectra yielded a diagnostic sensitivity of 93.5% and specificity of 97.8% for *in vivo* cervical cancer identification [17]. In this study RS gave a sensitivity and specificity of 91% and 96%, respectively for differentiating tumor (T) from normal (N) sites.

The specificity and PPV values obtained for DR and Raman in the present study are comparable (Table 3). However, the sensitivity and NPV were slightly lower for DR as compared to Raman. Since DR technique focuses on changes in oxygenated haemoglobin absorption changes, the lower sensitivity observed in this study could be attributed to bleeding noticed in tumor sites.

In the present study, RS has shown slightly improved diagnostic accuracy as compared to DR, but the RS system has a larger footprint and is costlier as compared to the DR device. Further, the fibre optic probe used in DRS is of low-cost and less complexity as compared to that used in Raman system and the white light used to record DR spectra could be a tungsten halogen lamp or LED source. RS system requires a dark room for recording of spectra and hence, is less suitable for field use. Therefore, RS systems would be ideally suited for centralised facilities or large hospitals. In comparison, the DR system is compact, light weight, low-cost and portable, and could therefore be ideally suited for field applications and community level screening programs.

Similar comparative studies were reported in the literature, but not on cervical cancer patients. Majumder et al. has reported an *ex vivo* study on 74 breast tissue samples for comparing the performance of autofluorescence, diffuse reflectance and Raman spectroscopy for discriminating different histopathologic categories of human breast tissues, which showed Raman spectroscopy to be superior in comparison to all others [59]. In another *ex vivo* study for targeted detection of breast lesions with microcalcifications, Soares et al. reported that the performance of the diffuse reflectance decision algorithm is comparable to the one derived from the corresponding Raman spectra, but the higher intensity of the reflectance signal enabled detection of lesions in a fraction of the spectral acquisition time [60]. Jayanti et al. compared the potential utility of autofluorescence and diffuse reflectance spectroscopy for clinical screening by collecting the spectral data from the same site of oral cancer patients [38]. Analysis of data recorded from 65 patients using PCA and LDA showed that the DRS has improved diagnostic accuracy as compared to autofluorescence for *in vivo* tissue classification.

In the light of the improvement in diagnostic accuracy achieved using PCA-LDA analytical techniques, the diffuse reflectance and spectroscopic mi-

croendoscope (DRSME) that has a series of collection fibers at the probe tip to record the diffuse reflectance spectra from deeper and deeper layers of tissue, can have improved diagnostic accuracies while interrogating deeper layers of tissue [61].

4. Conclusions

Both Raman and diffuse reflectance techniques are quantitative and non-invasive in nature and use fibre optic probes for easy access and screening of the whole cervix. The objective nature of the tests provides significant sensitivity and specificity as compared to traditional technologies such as the Pap smear and colposcopy directed biopsy. But the major deficiency is that point monitoring requires a larger time-frame to screen a larger area. Nonetheless, these “see and treat” methods could reduce the stress and anxiety of women and would be particularly beneficial in rural communities in the developing countries where an adequate health care infrastructure is not possible. Owing to the improved diagnostic accuracies, RS systems is the preferred choice for centralized facilities, whereas owing to lower cost and less complexity, the DR is more suited as a large-scale screening modality among rural communities.

In addition to the cervical cancer screening application, the DR system can be easily adapted for endoscopic screening of tissue linings of the gastrointestinal tract, the stomach or the colon by integrating any commercial endoscope with a miniature spectrometer and redesigning the probe tip to have the DR illumination/collection fiber at optimal separation, coupled to a micro-electro-mechanical scanner (MEMS) for point-to-point screening of the lesion and generating a 2D map in real-time.

Acknowledgements VGP was supported under the Faculty Improvement Program of the UGC, Govt. of India, at the NCESS, Thiruvananthapuram and she is thankful to the Director of the institute for providing facilities to undertake this research. The authors are also thankful to the technical staff at TMH, Mumbai for their assistance and support. The cooperation of all the patients enrolled for the clinical study is greatly appreciated.

Author biographies Please see Supporting Information online.

References

- [1] M. H. Stoler and M. Schiffman, *JAMA* **285**, 1500–1506 (2001).
- [2] R. A. Kerkar and Y. V. Kulkarni, *J. Obstet. Gynecol. India* **56**, 115–122 (2006).

- [3] D. Evers, B. Hendriks, G. Lucassen, and T. Ruers, *Future Oncol.* **8**, 307–320 (2012).
- [4] D. I. Ellis, D. P. Cowcher, L. Ashton, S. O'Hagan, and R. Goodacre, *Analyst*. **138**, 3871–3884 (2013).
- [5] H. Zeng, *Optics in the Life Sciences*, OSA Technical Digest (online) (Optical Society of America), paper BM2A.1. (2013).
- [6] Q. Tu and C. Chang, *Nanomedicine: Nanotechnology, Biology and Medicine* **8**, 545 (2012).
- [7] E. Brauchle and L. K. Schenke, *Biotechnol. J.* **8**, 288–297 (2013).
- [8] C. Krafft and V. Sergo, *Spectroscopy* **20**, 195–218 (2006).
- [9] M. B. Fenn, P. Xanthopoulos, G. Pyrgiotakis, S. R. Grobmyer, P. M. Pardalos, and L. L. Henchet, *Adv. Opt. Technol.* **2011**, 1–20 (2011).
- [10] P. Crow, A. Molckovsky, N. Stone, J. Uff, B. Wilson, and L. M. WongKeeSong, *Urology* **65**, 1126–1130 (2005).
- [11] A. Mahadevan-Jansen, N. Ramanujam, A. Malpica, S. Thomsen, U. Utzinger, and R. R. Kortum, *Photochem. Photobiol.* **68**, 123–132 (1998).
- [12] A. Mahadevan-Jansen, M. F. Mitchell, N. Ramanujam, U. Utzinger, and R. R. Kortum, *Photochem. Photobiol.* **68**, 427–431 (1998).
- [13] U. Utzinger, D. L. Heintzelman, A. Mahadevan-Jansen, A. Malpica, M. Follen, and R. R. Kortum, *Appl. spectroscopy* **55**, 955–959 (2001).
- [14] E. M. Kanter, E. Vargis, S. Majumder, M. D. Keller, E. Woeste, G. G. Rao, and A. Mahadevan-Jansen, *J. Biophoton.* **2**, 81–90 (2009).
- [15] E. M. Kanter, A. R. Viehoveer, G. J. Kanter, H. Shappell, H. W. Jones, and A. M. Jansen, *J. Raman Spectrosc.* **40**, 205–211 (2009).
- [16] E. M. Kanter, S. Majumder, G. J. Kanter, E. M. Woeste, and A. M. Jansen, *Am. J. Obstet. Gynecol.* **200**, 512E/1–512E/5 (2009).
- [17] J. Mo, W. Zheng, J. J. H. Low, J. Ng, A. Ilancheran, and Z. Huang, *Anal. Chem.* **81**, 8908–8915 (2009).
- [18] S. Duraipandian, W. Zheng, J. Ng, J. J. H. Low, A. Ilancheran, and Z. Huang, *Analyst*. **136**, 4328–4336 (2011).
- [19] S. Duraipandian, W. Zheng, J. Ng, J. J. H. Low, A. Ilancheran, and Z. Huang, *Anal. Chem.* **84**, 5913–5919 (2012).
- [20] S. Duraipandian, W. Zheng, J. Ng, J. J. H. Low, A. Ilancheran, and Z. Huang, *J. Biomed. Opt.* **18**(6), 067007 (2013).
- [21] S. Rubina, T. K. Dora, S. Chopra, A. Maheshwari, D. K. Kedar, R. Bharat, and C. M. Krishna, *J. Biomed. Opt.* **19**, 087001–087008 (2014).
- [22] S. Rubina, P. Sathae, T. K. Dora, S. Chopra, A. Maheshwari, D. K. Kedar, R. Bharat, and C. M. Krishna, *Proc. SPIE, Opt. Biopsy XII* **8940**, 89400E/1–89400E/6 (2014).
- [23] S. Rubina and C. M. Krishna, *J. Cancer Res. Ther.* **11**, 10–17 (2015).
- [24] N. Subhash, J. R. Mallia, S. S. Thomas, A. Mathews, P. Sebastian, and J. Madhavan, *J. Biomed. Opt.* **11**, 014018–014023 (2006).
- [25] R. J. Mallia, S. S. Thomas, A. Mathews, R. Kumar, P. Sebastian, J. Madhavan, and N. Subhash, *J. Biomed. Opt.* **13**, 1–10 (2008).
- [26] J. L. Jayanthi, G. U. Nisha, S. Manju, E. K. Philip, P. Jeemon, K. V. Baiju, V. T. Beena, and N. Subhash, *BMJ open* **1**, 1–7 (2011).
- [27] U. Utzinger, M. Brewer, E. Silva, D. Gershenson, B. R. C. M. Follen Jr., and R. R. Kortum, *Lasers Surg. Med.* **28**, 56–66 (2001).
- [28] Y. N. Mirabal, S. K. Chang, E. N. Atkinson, A. Malpica, M. Follen, and R. R. Kortum, *J. Biomed. Opt.* **7**, 587–594 (2002).
- [29] R. J. Nordstrom, L. Burke, J. M. Niloff, and J. F. Myrtle, *Lasers Surg. Med.* **29**, 118 (2001).
- [30] S. K. Chang, Y. N. Mirabal, E. N. Y. N. Atkinson, D. Cox, A. Malpica, M. Follen, and R. R. Kortum, *J. Biomed. Opt.* **10**, 024031–024041 (2005).
- [31] I. Georgakoudi, E. E. Sheets, M. G. Müller, V. Backman, C. P. Crum, K. Badizadegan, R. R. Dasari, and M. S. Feld, *Am. J. Obstet. Gynecol.* **186**, 374–382 (2002).
- [32] C. Zhu, G. M. Palmer, T. M. Breslin, J. Harter, and N. Ramanujam, *J. Biomed. Opt.* **13**, 034015–034030 (2008).
- [33] G. M. Palmer, C. Zhu, T. M. Breslin, F. Xu, W. K. Gilchrist, and N. Ramanujam, *Appl. Opt.* **45**, 1072–1078 (2006).
- [34] Z. Volynskaya, A. S. Haka, K. L. Bechtel, M. Fitzmaurice, R. Shenk, N. Wang, J. Nazemi, R. R. Dasari, and M. S. Feld, *J. Biomed. Opt.* **13**, 024012–024020 (2008).
- [35] F. Koenig, R. Larne, H. Enquist, F. J. McGovern, K. T. Schomacker, N. Kollias, and T. F. Deutsch, *Urology* **51**, 342–346 (1998).
- [36] J. R. Mourant, T. J. Bocklage, T. M. Powers, H. M. Greene, M. H. Dorin, A. G. Waxman, M. M. Zsemlye, and H. O. Smith, *J. Low Genit. Tract. Dis.* **13**, 216–223 (2009).
- [37] R. J. Mallia, N. Subhash, J. Madhavan, P. Sebastian, R. Kumar, A. Mathews, G. Thomas, and J. Radhakrishnan, *Appl. Spectrosc.* **64**, 409–418 (2010).
- [38] J. L. Jayanthi, N. Subhash, M. Stephen, E. K. Philip, and V. T. Beena, *J. Biophoton.* **4**, 696–706 (2011).
- [39] V. G. Prabitha, S. Suchetha, J. L. Jayanthi, K. V. Baiju, P. Rema, K. Anuraj, A. Mathews, P. Sebastian, and N. Subhash, *Lasers Med. Sci.* DOI 10.1007/s10103-015-1829-z (2015).
- [40] D. G. Ferris, R. A. Lawhead, E. D. Dickman, N. Holtzapple, J. A. Miller, S. Grogan, S. Bambot, A. Agrawal, and M. L. Faupel, *J. Low Genit. Tract. Dis.* **5**, 65–72 (2001).
- [41] A. M. Siddiqi, H. Li, F. Faruque, W. Williams, K. Lai, M. Hughson, S. Bigler, J. Beach, and W. Johnson, *Cancer* **114**, 13–21 (2008).
- [42] V. G. Prabitha, S. Suchetha, J. L. Jayanthi, P. Rema, K. V. Baiju, S. Nita, M. Anita, P. Sebastian, and N. Subhash, *IJESIT* **3**, 169–177 (2014).
- [43] B. Yu, A. Shah, V. K. Nagarajan, and D. G. Ferris, *Biomed. Opt. Express* **5**, 675–689 (2014).
- [44] M. C. Pierce, Y. Guan, M. K. Quinn, X. Zhang, W. H. Zhang, Y. L. Qiao, P. Castle, and R. R. Kortum, *Cancer Prev. Res. (Phila)* **5**, 1273–1279 (2012).

- [45] S. Wang and X. Zhou, Spectroscopic sensor on mobile phone, Patent No. US7420663, (2008).
- [46] C. Gobinet, V. Vrabie, M. Manfait, and O. Piot, *IEEE Trans. Biomed. Eng.* **56**, 1342–1371 (2009).
- [47] A. Nijssen, K. Maquelin, L. F. Santos, P. J. Caspers, T. C. B. Schut, J. C. den Hollander, M. H. Neumann, and G. J. Puppels, *J. Biomed. Opt.* **12**, 034004–034010 (2007).
- [48] S. Koljenovic, L. P. Choo-Smith, T. C. Bakker Schut, J. M. Kros, H. J. van den Berge, and G. J. Puppels, *Lab. Invest.* **82**, 1265–1277 (2002).
- [49] A. Ghanate, S. Kothiwale, S. P. Singh, D. Bertrand, and C. M. Krishna, *J. Biomed. Opt.* **16**(2), 025003 (2011).
- [50] A. Wang, V. Nammalavar, and R. Drezek, *J. Biomed. Opt.* **12**, 044012 (2007).
- [51] D. S. Ferreira, P. G. Coutinho, E. S. Castanheira, J. H. Correia, and G. Minas, *Conf. Proc. IEEE Eng. Med. Biol. Soc.* 1210–1213 (2010).
- [52] W. Kemmner, K. Wan, S. Rüttinger, B. Ebert, R. Macdonald, U. Klamm, and K. T. Moesta, *FASEB J.* **22**, 500–509 (2008).
- [53] A. Amelink, H. J. Sterenborg, M. P. Bard, and S. A. Burgers, *Opt. Lett.* **29**, 1087–1089 (2004).
- [54] L. B. Lovat, K. Johnson, G. D. Mackenzie, B. R. Clark, M. R. Novelli, S. Davies, M. O'Donovan, C. Selvasekar, S. M. Thorpe, D. Pickard, R. Fitzgerald, T. Fearn, I. Bigio, and S. G. Bown, *Gut.* **55**, 1078–1083 (2006).
- [55] G. Socrates, *Infrared and Raman Characteristic Group Frequencies: Tables and Charts-3rd edition*, John Wiley & Sons (2004).
- [56] C. M. Krishna, G. D. Sockalingum, G. Kegelaer, S. Rubin, B. Vasudevan, V. B. Kartha, and M. Manfait, *Vib. Spectrosc.* **38**, 95–100 (2005).
- [57] C. M. Krishna, N. B. Prathima, R. Malini, B. M. Vadhiraaja, R. A. Bhatt, D. J. Fernandes, P. Kushtagi, M. S. Vidyasagar, and V. B. Kartha, *Vib. spectrosc.* **41**, 136–141 (2006).
- [58] B. Young, G. O'Dowd, and P. Woodford, *Wheater's functional histology: a text and colour atlas*, Chapter 19 in *Female Reproductive System*, pp. 351–383, Elsevier, USA (2006).
- [59] S. K. Majumder, M. D. Keller, F. I. Boulos, M. C. Kelley, and J. A. Mahadevan, *J. Biomed. Opt.* **13**, 054009 (2008).
- [60] J. S. Soares, I. Barman, N. C. Dingari, Z. Volynskaya, W. Liu, N. Klein, D. Plecha, R.R. Dasari, and M. Fitzmaurice, *PNAS* **110**, 471–476 (2013).
- [61] G. J. Greening, A. J. Powless, J. A. Hutcheson, S. P. Prieto, A. A. Majid, and T. J. Muldoon, *Proc. SPIE Int. Soc. Opt. Eng.* **9332**, 93320R (2015).